International Journal of Coal Geology 83 (2010) 446–455

Contents lists available at ScienceDirect

International Journal of Coal Geology

journal homepage: www.elsevier.com/locate/ijcoalgeo

Evaluation of stress-controlled coal swelling processes

Jishan Liu [a,*], Zhongwei Chen [a], Derek Elsworth [c], Xiexing Miao [b], Xianbiao Mao [b]

[a] Shool of Mechanical Engineering, The University of Western Australia, WA, 6009, Australia
[b] State Key Laboratory for Geomechanics and Underground Engineering, China University of Mining and Technology, China
[c] Department of Energy and Mineral Engineering, Penn State University, PA 16802-5000, USA

ARTICLE INFO

Article history:
Received 9 February 2010
Received in revised form 24 June 2010
Accepted 25 June 2010
Available online 1 July 2010

Keywords:
Coal–gas interactions
Stress-controlled sorption
Coal swelling
Coal permeability
Numerical modeling

ABSTRACT

Stress-controlled swelling tests are normally conducted in the laboratory to characterize the evolution of coal permeability under the influence of gas sorption. Typically reductions in permeability are observed from gas-sorption-induced swelling even where effective stresses remain constant. This behavior remains enigmatic as the permeability of the porous coal is determined by the effective stress only. When these observations were interpreted, a matchstick or cubic coal model was assumed. Under this assumption, matrix swelling would not affect coal permeability because of the complete separation between matrix blocks caused by through-going fractures. This is why current coal permeability models have little success in explaining this inconsistency. It is generally believed that the reason for the failure is the inconsistency between the experimental conditions and the model assumptions. However, in this paper, it is considered that the reason may be the internal actions between coal fractures and matrixes have not been taken into consideration. In this study, a model capable of replicating this apparently anomalous behavior is developed. We consider the interactions of the fractured coal mass where cleats do not create a full separation between adjacent matrix blocks but where solid rock bridges are present. We accommodate the role of swelling strains both over contact bridges that hold cleat faces apart but also over the non-contacting span between these bridges. The effects of swelling act competitively over these two components: increasing porosity and permeability due to swelling of the bridging contacts but reducing porosity and permeability due to the swelling of the intervening free-faces. Under these conditions, a new permeability model is formulated. The new model is the key cross link that couples the multiphysics of coal–gas interactions. The formulation and incorporation of this permeability model into the multiphysics simulation of coal–gas interactions are presented in this paper.

1. Introduction

Knowledge of how gas sorption-induced changes in effective stresses affect the permeability of coal is crucially important not only to operations involving the production of natural gas from coalbeds, but also to the design and operation of projects to sequester greenhouse gases in coalbeds (van Bergen et al., 2009). The potential impacts of coal swelling on the evolution of coal permeability have been investigated through experimental, field-scale, and numerical studies.

Changes in permeability of coal cores confined under isotropic stresses show that desorption of an adsorbing gas, such as methane, accompany matrix shrinkage (Harpalani and Schraufnagel, 1990; Harpalani and Chen, 1997) and may result in a net permeability increase. Measurements of the effects of coal shrinkage have been carried out for the injection of different gases and the implications for cleat permeability change have been evaluated using a matchstick geometry model (Seidle and Huitt, 1995). These studies determine the change in coal permeability and volumetric strain rate as a result of gas pressure and suggest that swelling induced deformations dominate over effective-stress-generated deformations at low gas pressures for both carbon dioxide and methane. Similar results are available for measurements on coal samples in a triaxial stress permeameter (Wang et al., 2007).

More recently measurements of carbon dioxide permeability on an induced longitudinal fracture in coal have explored the impact of confining stress (Siriwardane et al., 2009). To avoid possible permeability change due to gas adsorption-induced coal swelling, permeabilities measured under constant gas pressure but with variable confining pressure have allowed comparison with Palmer and Mansoori and Shi and Durucan permeability models (Robertson, 2005; Pan et al., 2010). Similar work shows an increase in permeability with decreasing effective pressure on the sample when a non-sorbing gas is used but a reduction in permeability with increasing effective stress when an adsorbing gas is used (Pini et al.,

* Corresponding author.
E-mail address: jishan@cyllene.uwa.edu.au (J. Liu).

0166-5162/$ – see front matter © 2010 Elsevier B.V. All rights reserved.
doi:10.1016/j.coal.2010.06.005

2009). This observed switch in behavior is presumably due to the influence of the swelling on cleat deformation.

Other laboratory experiments have measured the change of coal permeability as a function of pore pressure and injected-gas composition at constant effective stress (Lin et al., 2008). The effect of CO_2 injection on the permeability of coal samples has been investigated with a high-pressure core flooding apparatus by imposing a constant effective stress on the sample (Mazumder et al., 2006; Mazumder and Wolf, 2008). Injection of CO_2 resulted in an observed increase in permeability even with absorbable gases including CO_2, CH_4 and N_2. Chemical and thermodynamic aspects of coal swelling due to solvents have been reported in the literature (Cody et al., 1988; Larsen et al., 1997; Kelemen et al., 2005) together with the potential influence of CO_2 injection to enhance coalbed methane recovery. These studies indicate that coal undergoes simultaneous swelling and shrinkage when carbon dioxide is injected into a coal seam to displace and recover the methane (Reeves and Oudinot, 2005; Mazumder et al., 2006).

More recently, a set of experiments have been carried out by Han et al. (2010) to measure the fluid conductivity properties of the coal matrix regarding both single phase (water) and two-phase (water and gas) fluid flow tests on a cylindrical anthracite coal matrix plug. The maximum effective permeability, with the value of 18 nDarcy was measured. Another different measures has been conducted by Huy et al. (2010) recently with a new procedure and methodology to estimate the fracture width in coal core samples, which was estimated from measurements of gas flow rates in a limited small area using a pipe attachment on the end of the surface of the core, and presented a linear relationship between fracture permeability and matrix permeability.

Based on experimental observations, a variety of models have been formulated to quantify the evolution of permeability during coal swelling/shrinkage. Gray (1987) firstly attempted to quantify the role of stresses on the evolution of coal-reservoir permeability, in which permeability was computed as a function of reservoir pressure-induced coal-matrix shrinkage assumed directly proportional to changes in the equivalent sorption pressure. Since then, a number of theoretical and empirical permeability models have been proposed (Seidle and Huitt, 1995; Palmer and Mansoori, 1996; Gilman and Beckie, 2000; Pekot and Reeves, 2002; Shi and Durucan, 2004; Cui and Bustin, 2005). However, most of these studies are under the assumption of either an invariant total stress or uniaxial strain conditions. These critical and limiting assumptions have been relaxed in new models rigorously incorporating in-situ stress conditions (Zhang et al., 2008; Connell, 2009; Palmer, 2009) and are extended to rigorously incorporate CO_2–CH_4 coal–gas interaction relevant to CO_2-ECBM (Connell and Detournay, 2009; Chen et al., 2010).

When experimental results from these tests are interpreted, a matchstick or cubic coal model is typically assumed with matrix block completely separated from each other in a stacked structure. Under this assumption, matrix swelling without any change in effective stress should not affect coal permeability because of the complete separation between matrix blocks caused by through-going fractures (Liu and Rutqvist, 2010). Matrix blocks will swell but the compaction of the fracture will not change, and therefore permeability should not change. However, this is not consistent with laboratory observations that show significant effects of matrix swelling on coal permeability even under conditions of constant confining stress (Harpalani and Schraufnagel, 1990; Harpalani and Chen, 1997; Pini et al., 2009). In order to explain these anomalous observations, uniaxial strain models have been invoked but with little success (Harpalani and Chen 1995; Robertson and Christiansen, 2007). It is generally believed that the reason for this failure is the inconsistency between the experimental conditions and the model assumptions (Liu and Rutqvist, 2010). However, in this paper, it is considered that the reason for these failures may be the internal actions between coal fractures and matrix have not been appropriately taken into consideration.

It is generally believed that permeability values for the coal matrix are typically several orders of magnitude smaller than fracture permeability values (Robertson, 2005). Therefore, most researchers generally ignore coal-matrix permeability and attribute coal permeability directly to fracture permeability, and consider that diffusion is the main way for gas transport in matrix system. However, relevant previous studies concluded that multiphase flow processes within a coal matrix may have considerable effects on coalbed methane recovery processes, while these effects are largely ignored in current modeling practice (Wei et al., 2007; Liu and Rutqvist, 2010). Therefore, it may be important to investigate the coal permeability change by combining the effects both matrix and fracture systems.

In this study, it is assumed that both fracture compartments between coal bridges and coal matrix contribute to the resultant coal permeability. It is linked through the elastic reduction ratio and to be verified through the comparisons with experimental data and other widely used permeability models, like Shi-Durucan model (2004) and Gu-Chalaturnyk model (2005). The new model is the key cross coupling that couples the multiphysics of coal–gas interactions under stress-controlled conditions. The formulation and incorporation of this permeability model into the multiphysics simulation of coal–gas interactions is documented in the following.

2. Coal permeability analysis

The following introduces a concept of fracture-matrix interaction to address the dichotomy that under stress controlled conditions, coal permeability is shown to reduce with an increase in sorbing gas pressure rather than remain constant.

2.1. Conceptual model

In this study, it is assumed that coal matrix blocks are connected to each other by coal-matrix bridges, as illustrated in Fig. 1(a). Both matrix and bridges swell during gas adsorption. Matrix swelling tends to narrow the fracture opening while the swelling of the coal-matrix bridge tends to widen the fracture. The net change in fracture opening could be positive (increase) or negative (reduction), as illustrated in Fig. 1(b) and (c). Therefore, the permeability could decrease or increase. The change in fracture opening due to the swelling of a coal-matrix bridge can be defined as $\Delta b_b = 1/3 \cdot b\varepsilon_s$. The change in fracture opening due to matrix swelling can be defined as $\Delta b_m = (s\varepsilon_s)/3$. Because $\Delta b_b \ll \Delta b_m$, the net change in fracture opening due to free expansion would be negative. In other words, the existence of coal-matrix bridges will reduce the fracture (cleat) permeability.

For coal matrix permeability, because free expansion of coal matrix swelling/ shrinkage does not change coal matrix permeability, as shown in Fig. 2, the permeability for matrix system is controlled by the mechanical effective stress change only, i.e., $\sigma - p_m$. If the confining stress σ does not change, then the change in mechanical effective stress can be defined as $-\Delta p_m$. For fracture system, the permeability change is related to two factors: mechanical effective stress change and sorption-induced strain. The resultant change in coal permeability is a combined outcome of the reduction in fracture opening due to coal matrix swelling and the decrease in effective stress due to pore pressure change.

2.2. General theory for permeability

For general porous media system, the following two assumptions are considered: (1) the coal matrix system is a homogeneous, isotropic and elastic continuum, and the system is isothermal; and (2) strains are infinitesimal.

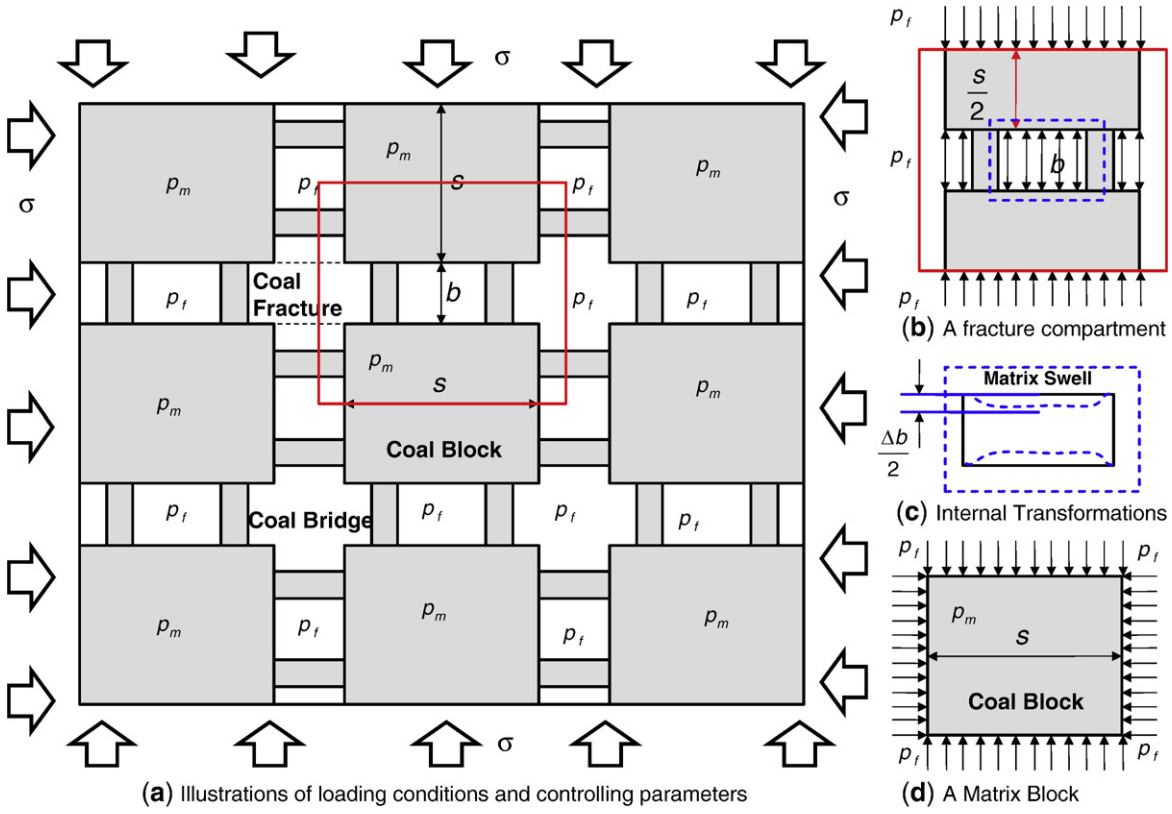

Fig. 1. Conceptual model for coal-matrix bridges.

The gas sorption-induced strain ε_s is assumed to result in only normal strains and these resulting strains are isotropic. The effects of gas sorption on the deformation of coal seams can be treated analogous to the effects of temperature for elastic porous media (e.g., Palmer and Mansoori, 1996), stress–strain relationships for an isothermal gas adsorbing coalbed may be written as (Zhang et al., 2008)

$$\varepsilon_{ij} = \frac{1}{2G}\sigma_{ij} - \left(\frac{1}{6G} - \frac{1}{9K}\right)\sigma_{kk}\delta_{ij} + \frac{\alpha}{3K}p\delta_{ij} + \frac{\varepsilon_s}{3}\delta_{ij} \quad (1)$$

where $G = \frac{E}{2(1+\nu)}$, $K = \frac{E}{3(1-2\nu)}$, $\alpha = 1 - \frac{K}{K_m}$, $\sigma_{kk} = \sigma_{11} + \sigma_{22} + \sigma_{33}$. E is the Young's modulus of the coal-fracture assemblage, K represents the bulk modulus coal-fracture assemblage, and K_m represents the bulk modulus of coal matrixes. G is the shear modulus of coal, ε_s is the sorption-induced strain, and ν is the Poisson's ratio of the coal-fracture assemblage. α represents the Biot's coefficient, p the gas pressure in the pores and δ_{ij} is the Kronecker delta; 1 for $i = j$ and 0 for $i \neq j$.

From Eq. (1), we obtain

$$\varepsilon_v = -\frac{1}{K}(\overline{\sigma} - \alpha p) + \varepsilon_s \quad (2)$$

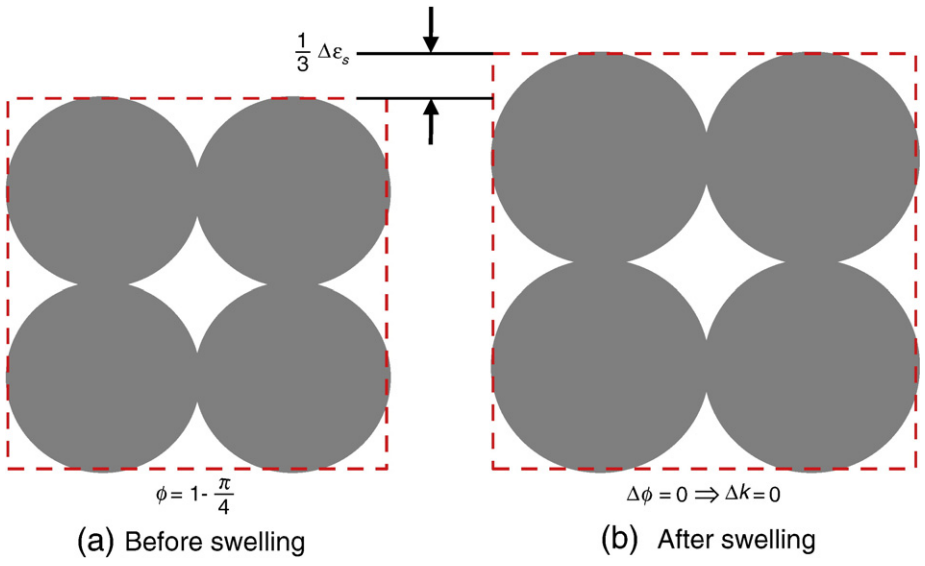

Fig. 2. Illustration of free expansion of coal matrixes.

where $\varepsilon_v = \varepsilon_{11} + \varepsilon_{22} + \varepsilon_{33}$ is the volumetric strain of the coal matrix and $\bar{\sigma} = \sigma_{kk}/3$ is the mean compressive stress. The effective stress σ_{eij} is defined as $\sigma_{eij} = \sigma_{ij} + \alpha p \delta_{ij}$.

Considering a porous medium containing solid volume of V_s and pore volume of V_p, we assume the bulk volume $V = V_p + V_s$ and the porosity $\phi = V_p / V$. According to Eq. (2), the volumetric evolution of the porous medium loaded by total stress $\bar{\sigma}$ and gas pressure p can be described in terms of $\Delta V / V$ and $\Delta V_p / V_p$, the volumetric strain of coal and volumetric strain of pore space, respectively. The relations are

$$\frac{\Delta V}{V} = -\frac{1}{K}(\Delta\bar{\sigma} - \alpha\Delta p) + \Delta\varepsilon_s \tag{3}$$

$$\frac{\Delta V_p}{V_p} = -\frac{1}{K_p}(\Delta\bar{\sigma} - \beta\Delta p) + \Delta\varepsilon_s \tag{4}$$

where $\beta = 1 - K_p / K_s$.

We assume that the sorption-induced strain for the coal is the same as for the pore space. Without the gas sorption effect, the volumetric variation of the porous medium satisfies the Betti-Maxwell reciprocal theorem, $\frac{\partial V}{\partial p}\Big|_{\bar{\sigma}} = \frac{\partial V_p}{\partial \bar{\sigma}}\Big|_p$, (Hudson et al., 1993) and we obtain

$$K_p = \frac{\phi}{\alpha} K. \tag{5}$$

Using the definition of porosity, the following expressions can be deduced as

$$\frac{\Delta V}{V} = \frac{\Delta V_s}{V_s} + \frac{\Delta\phi}{1-\phi} \tag{6}$$

$$\frac{\Delta V_p}{V_p} = \frac{\Delta V_s}{V_s} + \frac{\Delta\phi}{\phi(1-\phi)} \tag{7}$$

Solving Eqs. (3)–(7), we obtain the relationship as

$$\Delta\phi = \phi\left(\frac{1}{K} - \frac{1}{K_p}\right)(\Delta\bar{\sigma} - \Delta p) \tag{8}$$

$$\phi - \phi_0 = -(\alpha - \phi)\frac{(\Delta\bar{\sigma} - \Delta p)}{K}. \tag{9}$$

Rearranging the above equation gives

$$\phi = \frac{\phi_0}{\left(1 - \frac{\Delta\bar{\sigma} - \Delta p}{K}\right)} - \frac{\alpha}{\left(1 - \frac{\Delta\bar{\sigma} - \Delta p}{K}\right)}\frac{\Delta\bar{\sigma} - \Delta p}{K}. \tag{10}$$

Because generally $(\Delta\bar{\sigma} - \Delta p)/K \ll 1$, the above equation can be simplified into

$$\frac{\phi}{\phi_0} = 1 - \frac{\alpha}{\phi_0}\frac{\Delta\sigma - \Delta p}{K} = 1 + \frac{\alpha}{\phi_0}\Delta\varepsilon_{et} \tag{11}$$

where $\Delta\varepsilon_{et} = -(\Delta\bar{\sigma} - \Delta p)/K$ is defined as the total effective volumetric strain (negative sign represents compressive strain).

2.3. Permeability of coal matrix system

From Eq. (11) we can see that under stress-controlled boundary condition, the matrix porosity change can be expressed as:

$$\frac{\phi_m}{\phi_m 0} = 1 - \frac{1}{\phi_{m0}}\frac{\Delta\sigma - \Delta p_m}{K_m}. \tag{12}$$

It is clear that there is a relationship between porosity, permeability and grain-size distribution of porous medium. Chilingar et al. (1963) defined this relationship as

$$k = \frac{d_e^2 \phi^3}{72(1-\phi)^2} \tag{13}$$

where, k is the permeability, $\phi$is porosity and d_e is the effective diameter of grains. Based on this equation, we can obtain

$$\frac{k}{k_0} = \left(\frac{\phi}{\phi_0}\right)^3 \left(\frac{1-\phi_0}{1-\phi}\right)^2 \tag{14}$$

when the porosity is much smaller than 1 (Normally less than 10%), the second term of the right side can be ignored. Then we have the cubic relationship of permeability and porosity can be also use for matrix.

$$\frac{k}{k_0} = \left(\frac{\phi}{\phi_0}\right)^3 \tag{15}$$

Therefore, the permeability for coal matrix system can be given as

$$\frac{k_m}{k_{m0}} = \left(1 - \frac{1}{\phi_{m0}}\frac{\Delta\bar{\sigma} - \Delta p_m}{K_m}\right)^3 \tag{16}$$

2.4. Permeability of fracture compartments between coal bridges

For fracture system, the aperture determines that permeability value, as shown in Fig. 1. In order to calculate the fracture aperture variation due to mechanical effective stress change and coal matrix swelling/shrinkage, the following schematic diagram is drawn, as shown in Fig. 3. In the analysis of fracture aperture change, the fractured coal mass is replaced as an equivalent continuous medium, which has been supported by prior researches (Amadei and Goodman, 1981).

For fracture system, the aperture closure induced by the total effective stress change can be calculated by

$$\Delta b = (b + s)\cdot\frac{\Delta\sigma_{et}}{E} - s\cdot\frac{\Delta\sigma_{et}}{E_m} \tag{17}$$

Simplifying this equation, gives

$$\Delta b = s\cdot\left(1 - \frac{E}{E_m}\right)\frac{\Delta\sigma_{et}}{E} + b\cdot\frac{\Delta\sigma_{et}}{E} \tag{18}$$

If assuming $R_m = E / E_m$ and using $\Delta\varepsilon_{et}$ to represent $\Delta\sigma_{et} / E$ term, then the above equation can be derived

$$\Delta\varepsilon_f = \frac{\Delta b}{b} = \left[\frac{s\cdot(1-R_m)}{b} + 1\right]\cdot\Delta\varepsilon_{et} \tag{19}$$

Because $b \ll s$, the above equation can be simplified into

$$\Delta\varepsilon_f = \frac{\Delta b}{b} = \frac{s\cdot(1-R_m)}{b}\Delta\varepsilon_{et} \tag{20}$$

where R_m is the elastic modulus reduction ratio, s is the fracture spacing, b_0 is the initial fracture aperture, and $\Delta\varepsilon_{et}$ is the total effective strain change, which can be defined as

$$\Delta\varepsilon_{et} = \frac{\Delta\varepsilon_v}{3} - \frac{\Delta\varepsilon_s}{3} \tag{21}$$

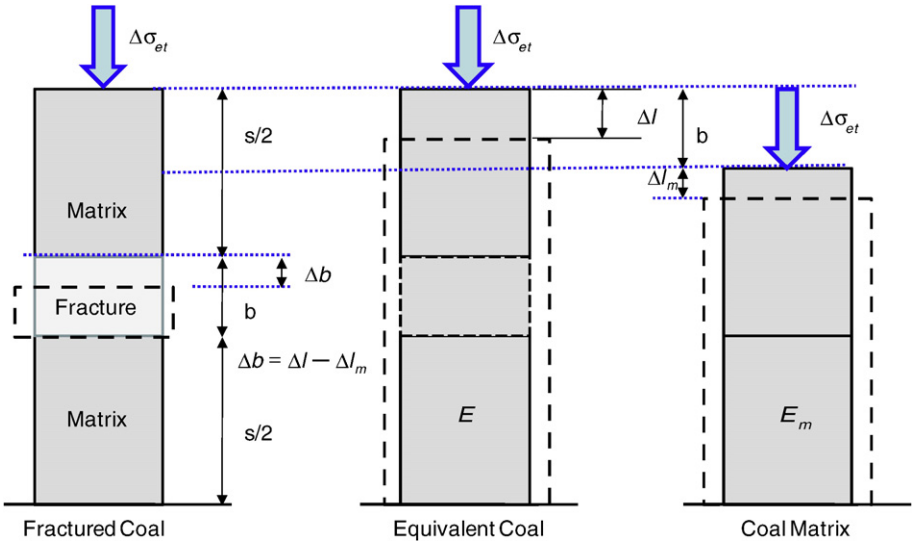

Fig. 3. Schematic diagram of fracture aperture interaction with effective stress.

The change in fracture opening can be defined as (Liu et al., 2010)

$$\frac{\Delta b}{b} = \frac{(1-R_m)}{\phi_{f0}}(\Delta\varepsilon_v - \Delta\varepsilon_s) \tag{22}$$

where $\Delta\varepsilon_v$ is the volumetric strain, and ϕ_{f0} is initial fracture porosity, defined as $\phi_{f0} = 3b/s$.

Then the fracture permeability can be expressed as

$$\frac{k_f}{k_{f0}} = \left(1 + \frac{\Delta b}{b}\right)^3 = \left[1 + \frac{(1-R_m)}{\phi_{f0}}(\Delta\varepsilon_v - \Delta\varepsilon_s)\right]^3 \tag{23}$$

2.5. Resultant permeability

The resultant change in coal permeability is a combined outcome of the reduction in fracture opening due to coal matrix swelling and effective stress change, as defined in Eq. (23) and the decrease in effective stress due change in fluid pressure and confining stress, as defined in Eq. (16). In this study, we assume that fracture and matrix deformation are both linear and fully recoverable, and deformations in normal closure or opening are the predominant permeability alteration mode. Therefore, coal permeability changes can be defined as a function of the variation of aperture through the elastic modulus reduction ratio, R_m. Correspondingly, it is assumed the permeability contributions from matrix and fracture are also regulated by R_m. When $R_m = 0$, it represents the case where fractures dominate the overall permeability; when $R_m = 1$, it represents the case where matrixes dominate the overall permeability. Under these assumptions, the resultant coal permeability is defined as (Van Golf-Racht, 1982)

$$k = k_m + k_f \tag{24}$$

$$\frac{k}{k_0} = \frac{k_{m0}}{k_{m0} + k_{f0}}\frac{k_m}{k_{m0}} + \frac{k_{f0}}{k_{m0} + k_{f0}}\frac{k_f}{k_{f0}}. \tag{25}$$

Substituting Eqs. (16) and (23) into Eq. (25) gives

$$\frac{k}{k_0} = \frac{k_{m0}}{k_{m0} + k_{f0}}\left(1 + \frac{R_m}{\phi_{m0}}\frac{p_m}{K}\right)^3 + \frac{k_{f0}}{k_{m0} + k_{f0}} \left[1 + \frac{(1-R_m)}{\phi_{f0}}(\Delta\varepsilon_v - \Delta\varepsilon_s)\right]^3. \tag{26}$$

In order to explain this model, the typical curves for different magnitudes of the elastic reduction ratio, R_m, are shown in Fig. 4. All other parameters used for the calculation are listed in Table 1.

3. Coupled model

3.1. Approach

The overall approach is illustrated in Fig. 5. The evaluation of fully-coupled deformation and gas transport in the fractured coal is conducted through four integrated steps: (1) Coal deformation analysis; (2) Flow equivalence analysis; (3) Permeability evolution analysis; and (4) Flow equivalence updating. These four steps are detailed in the following sections.

3.2. Coal deformation analysis

The mechanical properties of a discontinuous medium containing orthogonal fractures and anisotropic response can be represented by the properties of an equivalent continuous medium (Amadei and Goodman, 1981). The following considers the following assumptions:

(a) The coal is a homogeneous, isotropic and elastic continuum, and the system is isothermal.
(b) Strains are infinitesimal.

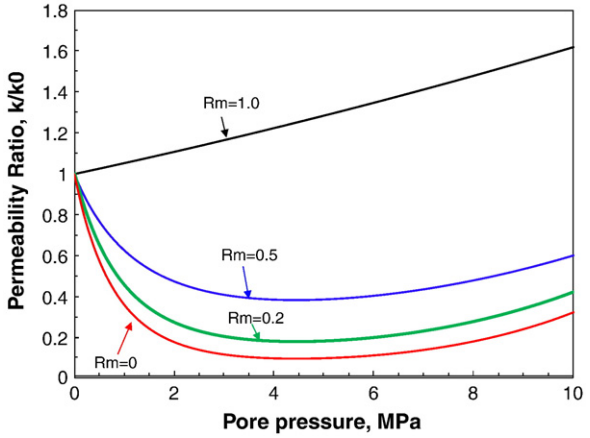

Fig. 4. Illustration of relations between the coal permeability ratio and the pore pressure under different magnitudes of R_m.

Table 1
Properties of coal cores measured in laboratory permeability experiments (Robertson, 2005).

Parameter	Definition	Value
E	Young's modulus, psi	200,000
k_{f0} / k_{m0}	Permeability ratio between two systems	100
k_0	Initial permeability, mD	0.0385
ϕ_{f0}	Initial fracture porosity	0.804%
ϕ_{m0}	Initial matrix porosity	5.0%
p_L	Langmuir pressure constant, psi	555.25
ε_L	Maximum volumetric sorption strain	0.01559

(c) Gas contained within the pores is ideal, and its viscosity is constant under isothermal conditions.
(d) Gas flow through the coal medium is assumed to be viscous flow obeying Darcy's law.

According to the first assumption (a), the strain–displacement relation is expressed as

$$\varepsilon_{ij} = \frac{1}{2}\left(u_{i,j} + u_{j,i}\right) \tag{27}$$

where ε_{ij} is the component of the total strain tensor and u_i is the component of the displacement. The equilibrium equation is defined as

$$\sigma_{ij,j} + f_i = 0 \tag{28}$$

where σ_{ij} denotes the component of the total stress tensor and f_i denotes the component of the body force.

Combining Eqs. (2) and (27)–(28) yields the Navier-type equation expressed as

$$G\nabla^2 u_i + \frac{G}{1-2\nu} e_{,i} - \alpha p_{,i} - K\varepsilon_{s,i} + f_i = 0 \tag{29}$$

where u_i is the displacement in i direction, e is the volumetric strain, and $p_{,i}$ is the partial derivative of pore pressure with respect to i. Eq. (29) is the governing equation representing deformation of the continuum representation of the fractured coal allowing deformations to be determined if fluid pressures, p, may be determined for both undrained and drained response. Transient fluid pressure is recovered from the flow equation.

For a system containing a single gas phase the sorption-induced volumetric strain ε_s may be represented by a Langmuir type function (Harpalani and Schraufnagel, 1990; Cui and Bustin, 2005; Robertson and Christiansen, 2007), defined as

$$\varepsilon_s = \varepsilon_L \frac{p}{P_L + p} \tag{30}$$

where ε_L and P_L are the Langmuir-type matrix swelling/shrinkage constants, which represent the maximum swelling capacity and the pore pressure at which the measured volumetric strain is equal to $0.5\varepsilon_L$, respectively. Both parameters are related with reservoir temperature.

$$G\nabla^2 u_i + \frac{G}{1-2\nu} e_{,i} - \alpha p_{,i} - \frac{K\varepsilon_L P_L}{(p + P_L)^2} p_{,i} + f_i = 0 \tag{31}$$

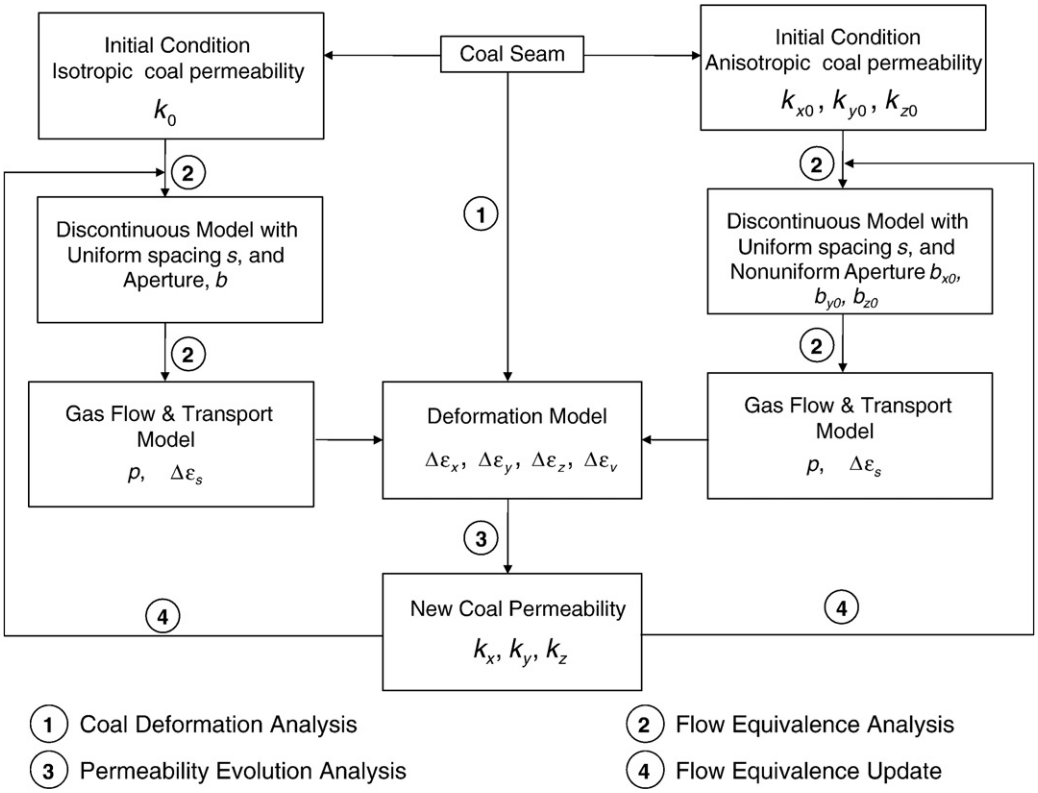

Fig. 5. Flow chart for evaluating coupled deformation and gas transport processes in coal. Circled numbers represent steps of the analysis process.

3.3. Flow and transport process

The mass balance equation for a single component gas is defined as

$$\frac{\partial m}{\partial t} + \nabla\cdot\left(\rho_g q_g\right) = Q_s \tag{32}$$

where ρ_g is the gas density, q_g is the Darcy velocity vector and Q_s is the gas source or sink. m is the gas content including both free-phase and absorbed components (Saghafi et al., 2007) and is defined as

$$m = \rho_g\left(\phi_m + \phi_f\right) + \left(1-\phi_m-\phi_f\right)\rho_{ga}\rho_c\frac{V_L p}{p+P_L} \tag{33}$$

where ρ_{ga} is the gas density at standard conditions, ρ_c is the coal density and ϕ_f is fracture porosity, ϕ_m is matrix porosity.

According to the real gas law, the gas density is proportional to the pore gas pressure and can be described as

$$\rho_g = \frac{M_g}{ZRT}p \tag{34}$$

where M_g is the molar mass of gas, R is the universal gas constant, T is the reservoir temperature and Z is the correction factor that accounts for the non-ideal behavior of the gas which changes with R and T.

From Eq. (11) we can see that the matrix porosity change regarding effective stress variation can be given as

$$\phi_m = \phi_{m0} - R_m\frac{\Delta\overline{\sigma}-\Delta p}{K} \tag{35}$$

From Eq. (22) we can know that fracture porosity change can be given as

$$\phi_f = \phi_{f0} + (1-R_m)(\Delta\varepsilon_v - \Delta\varepsilon_s) \tag{36}$$

Combining Eqs. (35) and (36) and submitting into Eq. (33) yields

$$\frac{\partial m}{\partial t} = \left[N\frac{\partial p}{\partial t} + (1-R_m)M\frac{\partial \varepsilon_v}{\partial t}\right]\left(\frac{M_g}{ZRT}\right) \tag{37}$$

where

$$M = p - p_a\rho_c\frac{V_L p}{p+p_L}$$

$$N = \left(\phi_m+\phi_f\right) - \frac{R_m}{K}M - (1-R_m)M\frac{\varepsilon_L p_L}{(p+p_L)^2} + \left(1-\phi_m-\phi_f\right)p_a\rho_c\frac{V_L p_L}{(p+p_L)^2}.$$

Substituting Eq. (37) into Eq. (32), yields the governing equation for gas flow through a coal seam with the effect of gas sorption incorporated as

$$N\frac{\partial p}{\partial t} - \nabla\cdot\left(\frac{\vec{k}}{\mu}p\nabla p\right) = -(1-R_m)M\frac{\partial \varepsilon_v}{\partial t} + Q_s \tag{38}$$

where μ denotes the dynamic viscosity of the gas and $\vec{k}$ denotes the permeability tensor, p_a is atmospheric pressure (1 atm. or 101.325 kPa).

3.4. Coupled model

By combining Eqs. (31) and (38) the fully coupled geomechanical and hydraulic flow processes model is developed. The third and fourth terms on the left-hand side of Eq. (31) represent the influence from pore pressure change and sorption-induced strain, respectively. The first term on the left-hand side of Eq. (38) represents all the controlling factors on porosity, including the volume occupied by the free-phase gas, the volume occupied by the adsorbed phase gas,

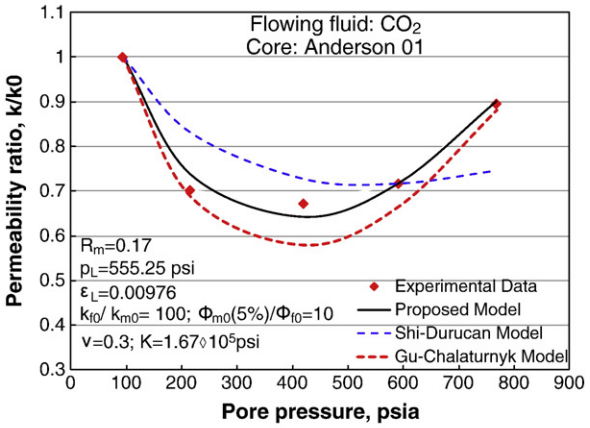

(a) Matching experimental data of CO_2 for core Anderson 01.

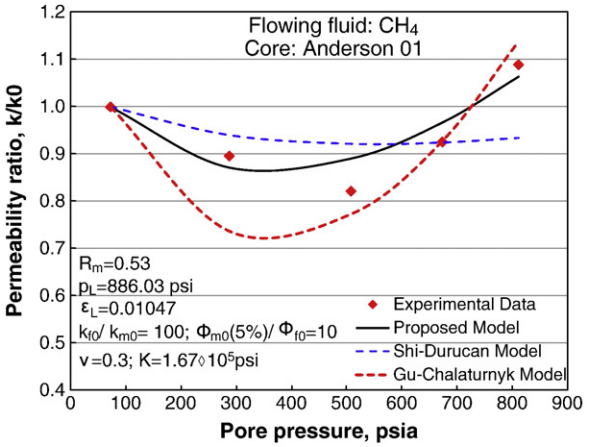

(b) Matching experimental data of CH_4 for Anderson 01.

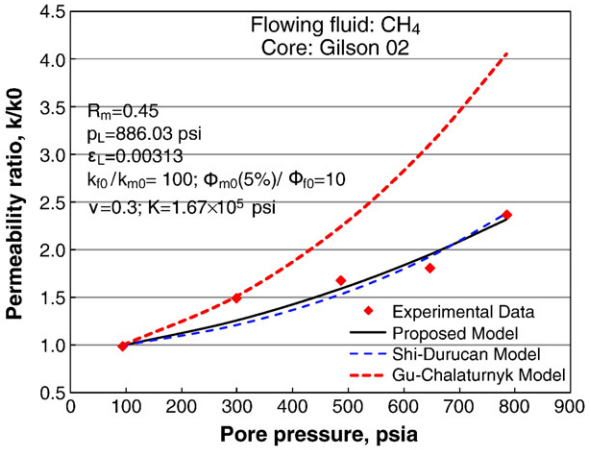

(c) Matching experimental data of CH_4 for core Gilson 02.

Fig. 6. Performances of different coal permeability models against experimental data for two coal cores under a constant confining pressure of 1000 psia. (a) Matching experimental data of CO_2 for core Anderson 01. (b) Matching experimental data of CH_4 for Anderson 01. (c) Matching experimental data of CH_4 for core Gilson 02.

the coal mechanical deformation induced pore volume change, and the sorption induced coal pore volume change. More importantly, these factors are quantified under in-situ stress conditions. The second term on the left-hand side is associated with the characteristics of gas seepage. On the right-hand side, the second term is a coupled term including the rate change in the volumetric strain due to coal deformation. Its contribution to the equation can be treated as a source or sink from the mechanical deformation.

When flow analysis is conducted, the total effective strain can be partitioned from the equivalent medium between coal matrix and fracture systems. Only the partitioned strain for both systems contributes to the permeability change. $R_m = 1$ means that the equivalent medium modulus is equal to that for the coal matrix. In other words, there is no fracture in the coal. Conversely, $R_m = 0$ means that the coal matrix modulus is infinitely stiff in comparison to the equivalent medium modulus. In other words, the total equivalent strain is due to the fracture system only. Therefore, $1-R_m$ represents the ratio of the partitioned strain to the total equivalent strain for the fracture system. If $R_m = 1$, the partitioned strain for the fracture system is near zero and no change in permeability in fracture system is assumed to result. If $R_m = 0$, the partitioned strain for the fracture system is the full bulk strain observed and therefore a maximum resultant permeability change is induced.

The total effective strain is the difference between the total strain, as determined by the constrained boundary conditions, and the free swelling strain. Therefore, the boundary conditions also control the evolution of coal permeability.

4. Model verification and application

4.1. Comparison with other permeability models and experimental data

The proposed permeability model is used to match the experimental data under stress controlled conditions (Robertson, 2005; Liu and Rutqvist, 2010). The model performance is also compared with other permeability models, including Shi-Durucan (2004) and Gu-Chalatumyk model (2005). The data for two coal samples (Anderson 01 and Gilson 02; Robertson 2005) was adapted for these comparisons. The confining stress was 1000 psia (6.8 MPa) for all experiments and the injection gases are CO_2 and CH_4, respectively. In these comparisons, the physical properties like Young's modulus, Poisson's ratio and Langmuir pressure constant are directly from experiments (Robertson, 2005). For the comparisons, only swelling constant and R_m are adjustable for the newly developed permeability model. These parameters are also used for the Gu-Chalatumyk model. For the Shi-Durucan model, only the cleat compressibility is adjustable to achieve the best match. As shown in Fig. 6, our model performs reasonably well. Comparison results also show that the maximum swelling strain values for the match are much smaller than the lab measured ones. It can be interpreted that the only part of sorption-induced strain contributes on permeability change. It has been generally assumed that the sorption-induced strain is totally counteracted by the fracture aperture closure, which has been proved by several researchers that it could dramatically overestimate the contribution from swelling/shrinkage strain (Robertson 2005, Liu and Rutqvist, 2010) and could obtain the negative permeability values (Mazumder et al., 2006).

4.2. Evaluation of stress-controlled coal swelling processes

Based on the permeability model of Eq. (25), a coupled 3D numerical model is constructed to simulate the performance of gas injection under stress-controlled conditions (hydostatic stress condition for this example). Input parameters for this simulation are from the coal core Anderson 01 with CO_2 injection, as shown in Fig. 6(a). The maximum sorption capacity of 27 m^3/t (standard) was adapted (Pan et al., 2010) and the initial fracture permeability value for AUS-2 core was chosen (Huy et al., 2010), with the value of 10 mD. The core is 50.8 mm in diameter and 100 mm in length with CO_2 injection at the top side. A constant hydrostatic stress of 1000 psi (6.89 MPa) is applied around the boundary, as shown in Fig. 7. For the gas transport model, the coal sample is saturated initially with CO_2 and the initial pressure is 94 psi (0.65 MPa). A constant injection pressure boundary

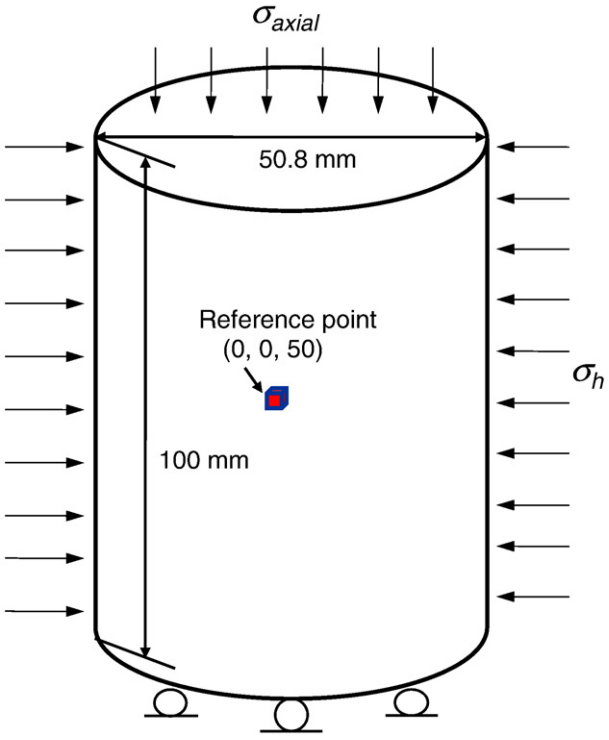

Fig. 7. Numerical simulation model under stress-controlled conditions.

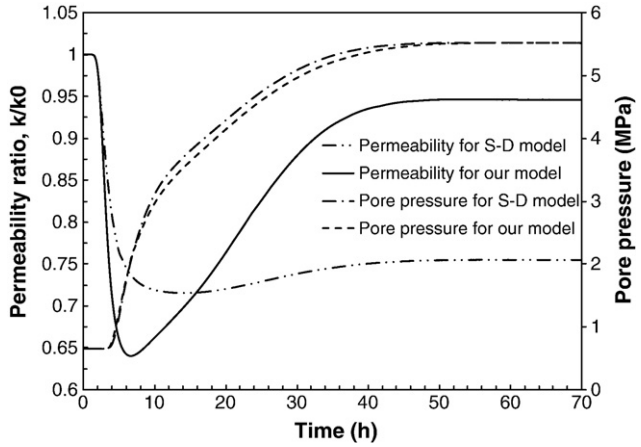

Fig. 8. Comparison of permeability ratio and pore pressure evolutions between our model and Shi-Durucan model.

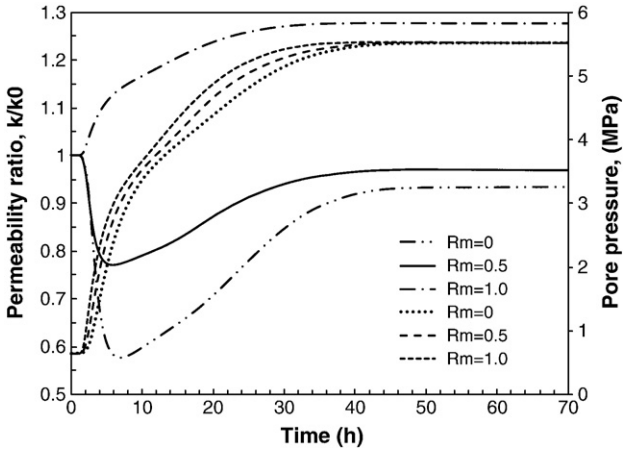

Fig. 10. Evolution of coal permeability and pore pressure for different values of R_m.

condition is specified at the top side of coal sample with the value of 800 psi (5.52 MPa), as shown in Fig. 7. This example is to investigate the transient permeability evolution with CO_2 injection, which is rarely measured under lab conditions. The comparisons between the proposed model and Shi-Durucan model are also carried out. The central point of the model was chosen as the reference point and simulation results are presented in Figs. 8–10.

The comparisons of permeability ratio and pore pressure evolutions between this developed permeability model and Shi-Durucan model are shown in Fig. 8. A significant difference of the permeability evolution for these two permeability models can be observed even under similar pore pressure profiles. This difference is due to the inconsistency between the S-D model assumptions and the boundary conditions for the simulation model.

The impact of k_{f0}/k_{m0} on the permeability and the pore pressure evolutions is shown in Fig. 9. In this study, $k_f = \frac{3}{\phi_{f0}} k_{f0} = 600 k_{f0}$. k_f, ϕ_{f0}, and k_{f0} are the individual fracture permeability, fracture porosity, and the fracture system permeability, respectively. Therefore, $k_f/k_{m0} = 600 k_{f0}/k_{m0}$. When $k_{f0}/k_{m0} = 1$ or $k_f/k_{m0} = 200$, it represents the coal fracture system permeability is equal to the coal matrix permeability. As this ratio increases, the permeability contribution from the matrix diminishes, which means that the importance of the fracture system enhances with the increase of this ratio. The dramatic difference also has been observed, as shown in Fig. 9 with the dotted lines.

The impact of R_m is shown in Fig. 10. When $R_m = 1$ or $1-R_m = 0$, it represents that the partitioned strain of the equivalent porous coal medium for the fracture system is zero. Under this condition, the coal fracture system has no contribution to the resultant coal permeability. When $R_m = 0$ or $1-R_m = 1$, it represents that the partitioned strain of the equivalent porous coal medium for the fracture system is 1. Under this condition, the coal matrix system has no contribution to the resultant coal permeability. Therefore $R_m = 0.5$ represents half of the total equivalent strain contributes to permeability change.

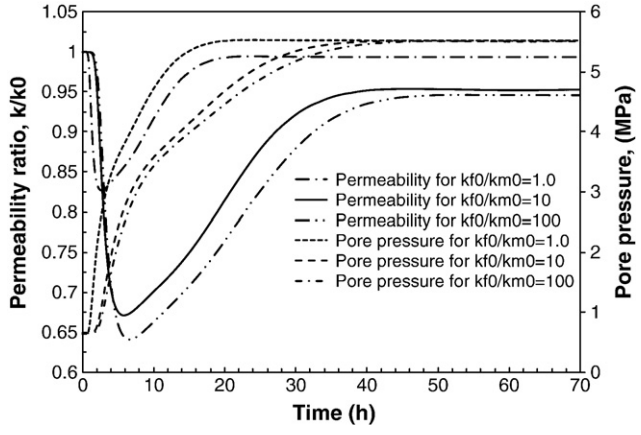

Fig. 9. Evolution of coal permeability and pore pressure under different magnitudes of the initial ratio of coal fracture permeability to matrix permeability (k_{f0}/k_{m0}).

5. Conclusions

A new permeability model has been developed to characterize the evolution of coal permeability under conditions of controlled stress, and implemented into a finite element model to quantify the multiphysics of coal–gas interactions. This may be applied both to represent laboratory data and field scale prototypes. Through model evaluations, the following conclusions can be drawn.

1. The new permeability model can be applied to explain the results from stress-controlled swelling tests. Stress-controlled swelling tests are normally conducted in the laboratory to characterize the evolution of coal permeability under the influence of gas sorption. When experimental results from these tests were interpreted, a matchstick or cubic coal model was assumed. Under this assumption, matrix swelling would not affect coal permeability because of the complete separation between matrix blocks caused by through-going fractures. However, this is inconsistent with laboratory observations that show significant effects of matrix swelling on coal permeability under constant confining stress conditions. Current coal permeability models have little success in explaining this inconsistency. It is generally believed that the reason for these failures is the inconsistency between the experimental conditions and the model assumptions. However the model presented here suggests that swelling of fracture faces may accommodate this failure and replicate a reduction in permeability, even under conditions of constant effective stress.
2. Results of the 3D simulation example show the importance of the consistency between assumptions of a coal permeability model and boundary conditions of a simulation model. Because the proposed coal permeability model in this study can be applied under a variety of stress conditions, it is best suitable to cases where coal deformation is rigorously considered.

Acknowledgements

This work was supported by the Western Australia CSIRO-University Postgraduate Research Scholarship, National Research Flagship Energy Transformed Top-up Scholarship, by NIOSH under

contract 200-2008-25702, and by State Key Laboratory for Geomechanics and Underground Geomechanics. These various sources of support are gratefully acknowledged.

References

Amadei, B., Goodman, R.E., 1981. A 3D constitutive relation for fractured rock masses. Proceedings of the International Symposium on the Mechanical Behavior of Structured Media, pp. 249–268.

Chen, Z., Liu, J., Elsworth, D., Connell, L.D., Pan, Z., 2010. Impact of CO_2 injection and differential deformation on CO_2 injectivity under in-situ stress conditions. International Journal of Coal Geology 81 (2), 97–108.

Chilingar, G.V., Main, R., Sinnokrot, A., 1963. Relationship between porosity, permeability, and surface areas of sediments. Journal of Sedimentary Research 33 (3), 759–765.

Cody, G.D., Larsen, J.W., Siskin, M., 1988. Anisotropic solvent swelling of coals. Energy and Fuels 2 (3), 340–344.

Connell, L.D., 2009. Coupled flow and geomechanical processes during gas production from coal seams. International Journal of Coal Geology 79 (1–2), 18–28.

Connell, L.D., Detournay, C., 2009. Coupled flow and geomechanical processes during enhanced coal seam methane recovery through CO_2 sequestration. International Journal of Coal Geology 77 (1–2), 222–233.

Cui, X., Bustin, R.M., 2005. Volumetric strain associated with methane desorption and its impact on coalbed gas production from deep coal seams. American Association of Petroleum Geologists Bulletin 89 (9), 1181–1202.

Gilman, A., Beckie, R., 2000. Flow of coal-bed methane to a gallery. Transport in Porous Media 41 (1), 1–16.

Gray, I., 1987. Reservoir engineering in coal seams: part 1 — the physical process of gas storage and movement in coal seams. SPE Reservoir Engineering 2 (1), 28–34.

Gu, F., Chalaturnyk, J.J., 2005. Analysis of Coalbed Methane Production by Reservoir and Geomechanical Coupling Simulation. Journal of Canadian Petroleum Technology 44 (10).

Han, F., et al., 2010. Experimental study of gas and water transport processes in the inter-cleat (matrix) system of coal: anthracite from Qinshui Basin, China. International Journal of Coal Geology 81 (2), 128–138.

Harpalani, S., Chen, G., 1995. Estimation of changes in fracture porosity of coal with gas emission. Fuel 74 (10), 1491–1498.

Harpalani, S., Chen, G., 1997. Influence of gas production induced volumetric strain on permeability of coal. Geotechnical and Geological Engineering 15 (4), 303–325.

Harpalani, S., Schraufnagel, R.A., 1990. Shrinkage of coal matrix with release of gas and its impact on permeability of coal. Fuel 69 (5), 551–556.

Hudson, J.A., Fairhurst, C., et al., 1993. Comprehensive rock engineering: principles, practice, and projects. Analysis and Design Method, Vol. II. Pergamon Press, Oxford, pp. 113–171.

Huy, P.Q., Sasaki, K., Sugai, Y., Ichikawa, S., 2010. Carbon dioxide gas permeability of coal core samples and estimation of fracture aperture width. International Journal of Coal Geology 83 (1), 1–10.

Kelemen, S.R., Kwiatek, L.M., Siskin, M., Lee, A.G.K., 2005. Structural response of coal to drying and pentane sorption. Energy and Fuels 20 (1), 205–213.

Larsen, J.W., Flowers, R.A., Hall, P.J., Carlson, G., 1997. Structural rearrangement of strained coals. Energy and Fuels 11 (5), 998–1002.

Lin, W., Tang, G.-Q., Kovscek, A.R., 2008. Sorption-induced permeability change of coal during gas-injection processes. SPE Reservoir Evaluation & Engineering 11 (4), 792–802.

Liu, H.-H., Rutqvist, J., 2010. A new coal-permeability model: internal swelling stress and fracture–matrix interaction. Transport in Porous Media 82 (1), 157–171.

Liu, J., Chen, Z., Elsworth, D., Miao, X., Mao, X., 2010. Linking gas-sorption induced changes in coal permeability to directional strains through a modulus reduction ratio. International Journal of Coal Geology 83 (1), 21–30.

Mazumder, S., Wolf, K.H., 2008. Differential swelling and permeability change of coal in response to CO_2 injection for ECBM. International Journal of Coal Geology 74 (2), 123–138.

Mazumder, S., Karnik, A.A., Wolf, K.-H.A.A., 2006. Swelling of coal in response to CO_2 sequestration for ECBM and its effect on fracture permeability. SPE Journal 11 (3), 390–398.

Palmer, I., 2009. Permeability changes in coal: analytical modeling. International Journal of Coal Geology 77 (1–2), 119–126.

Palmer, I., Mansoori, J., 1996. How Permeability Depends on Stress and Pore Pressure in Coalbeds. A New Model, SPE Annual Technical Conference and Exhibition. Society of Petroleum Engineers, Inc, Denver, Colorado. Copyright 1996.

Pan, Z., Connell, L.D., Camilleri, M., 2010. Laboratory characterisation of coal reservoir permeability for primary and enhanced coalbed methane recovery. International Journal of Coal Geology 82 (3–4), 252–261.

Pekot, L.J., Reeves, S.R., 2002. Modeling the effects of matrix shrinkage and differential swelling on coalbed methane recovery and carbon sequestration. U.S. Department of Energy DE-FC26-00NT40924. .

Pini, R., Ottiger, S., Burlini, L., Storti, G., Mazzotti, M., 2009. Role of adsorption and swelling on the dynamics of gas injection in coal. Journal of Geophysical Research 114 (B4), B04203.

Reeves, S., Oudinot, A., 2005. The Allison CO_2-ECBM Pilot, a reservoir and economic analysis coal. Proceedings of the International Coalbed Methane Symposium. Tuscaloosa, AL, U.S.A. May 17–19.

Robertson, E.P., 2005. Modeling Permeability in Coal Using Sorption-Induced Strain Data. SPE Annual Technical Conference and Exhibition. Society of Petroleum Engineers, Dallas, Texas.

Robertson, E.P., Christiansen, R.L., 2007. Modeling laboratory permeability in coal using sorption-induced strain data. SPE Reservoir Evaluation & Engineering 10 (3), 260–269.

Saghafi, A., Faiz, M., Roberts, D., 2007. CO_2 storage and gas diffusivity properties of coals from Sydney Basin, Australia. International Journal of Coal Geology 70 (1–3), 240–254.

Seidle, J.R., Huitt, L.G., 1995. Experimental Measurement of Coal Matrix Shrinkage Due to Gas Desorption and Implications for Cleat Permeability Increases, International Meeting on Petroleum Engineering. Society of Petroleum Engineers, Inc, Beijing, China. Copyright 1995.

Shi, J.Q., Durucan, S., 2004. Drawdown induced changes in permeability of coalbeds: a new interpretation of the reservoir response to primary recovery. Transport in Porous Media 56 (1), 1–16.

Siriwardane, H., Haljasmaa, I., McLendon, R., Irdi, G., Soong, Y., Bromhal, G., 2009. Influence of carbon dioxide on coal permeability determined by pressure transient methods. International Journal of Coal Geology 77 (1–2), 109–118.

van Bergen, F., Spiers, C., Floor, G., Bots, P., 2009. Strain development in unconfined coals exposed to CO_2, CH_4 and Ar: effect of moisture. International Journal of Coal Geology 77 (1–2), 43–53.

Van Golf-Racht, T.D., 1982. Fundamentals of fractured reservoir engineering. Elsevier Scientific Publishing. Company, Amsterdam.

Wang, F.Y., Zhu, Z.H., Massarotto, P., Rudolph, V., 2007. Mass transfer in coal seams for CO_2 sequestration. AIChE Journal 53 (4), 1028–1049.

Wei, X.R., Wang, G.X., Massarotto, P., Golding, S.D., Rudolph, V., 2007. A review on recent advances in the numerical simulation for coalbed–methane-recovery process. SPE Reservoir Evaluation & Engineering 10 (6), 657–666.

Zhang, H., Liu, J., Elsworth, D., 2008. How sorption-induced matrix deformation affects gas flow in coal seams: a new FE model. International Journal of Rock Mechanics and Mining Sciences 45 (8), 1226–1236.